

GLOBAL ACADEMIC RESEARCH INSTITUTE

COLOMBO, SRI LANKA



GARI International Journal of Multidisciplinary Research

ISSN 2659-2193

Volume: 08 | Issue: 03

On 30th September 2022

<http://www.research.lk>

Author: Luqmaan Rizan, Heshani Mudalige, Ominda perera

School of Science, BMS, Sri Lanka

GARI Publisher | Non-Communicable Disease | Volume: 08 | Issue: 03

Article ID: IN/GARI/ICAS/2022/123 | Pages: 75-90 (16)

ISSN 2659-2193 | Edit: GARI Editorial Team

Received: 17.07.2022 | Publish: 30.09.2022

IDENTIFICATION OF EFFECTIVE PHYTOCHEMICALS AGAINST NON-SMALL LUNG CANCER RECEPTOR USING AUTODOCK 4.2.6 SITE-SPECIFIC TECHNIQUE

Luqmaan Rizan, Heshani Mudalige, Ominda perera

School of Science, BMS, Sri Lanka

ABSTRACT

Lung cancer is a disease in which malignant cells develop in the tissues of the lungs, with an estimated 2 million diagnoses in 2020. Currently, no available drug can cure lung cancer, with no adverse side effects. This study was performed, to establish phytochemicals that can target the EFGR receptor tyrosine kinase domain with 4-anilinoquinazoline inhibitor erlotinib (PDB ID: 1M17), which was retrieved from RCSB PDB. 3D structures of 15 phytochemicals, were then retrieved using PubChem. ADMETlab 2.0 was also used to apply Lipinski's rule of five to examine the drug-likeness property. Receptor-Ligand specific-docking was performed using Autodock 4.2.6. The grid box parameters were set by choosing the active amino acid residues in the binding pocket retrieved using CASTp (ASP783, ASN784, GLN958, ARG962, MET963, HIS964, LEU977, MET978, ASP979, GLU980, ASP982, MET983, ASP984, and VAL986) of the receptor and the centre grid box values; X (20.663), Y (0 4.2060), and Z (56.92). BIOVIA DS and Chimera were used to determine the interactions and docking poses. Furthermore, validation was performed by redocking and obtaining a BE value of -6.15 kcal/mol. The effectiveness of the phytochemicals was gleaned from binding energy (BE) and inhibition constant (Ki). The best phytochemical of the 15 observed in this study was Ursolic acid based on BE, Ki, drug-likeness, and other scores (BE: -12.56 kcal/mol, Ki: 620.13 pM). Other

prospective phytochemicals are Phytosterols (BE: -9.87 kcal/mol), Nimbolide (BE: -7.95 kcal/mol), and Sparstolonin B (BE: -7.01 kcal/mol). Thus, these phytochemicals could be used to develop anti-cancer drugs, without any detrimental effects.

Keywords: Lung Cancer, tyrosine kinase domain with 4-anilinoquinazoline inhibitor erlotinib, Anti-cancer, Site-specific, Docking, Ursolic acid, EFGR.

INTRODUCTION

Multiple genetic and epigenetic alterations, such as the activation of growth-promoting pathways and the downregulation of tumor-suppressing pathways, contribute to the multi-step process that leads to lung cancer. The activation of growth-promoting proteins like the epidermal growth factor receptor (EGFR) and the inactivation of tumor suppressor genes are linked to oncogenesis in lung cancer, as in other malignancies. (Wistuba and Gazdar, 2006) At least 40–60 carcinogens are present in tobacco smoke. These substances damage DNA, which leads to somatic mutations in oncogenes and tumor suppressor genes. (Imyanitov et al., 2005) Following lung cancer (18.0% of all cancer-related deaths), colorectal cancer (9.4%), liver (8.3%), stomach (7.7%), and female breast cancer (6.9%) are the other frequent cancers. (Sung et al., 2021) The rate of

incidence and mortality for different cancers is available in Figure 01.

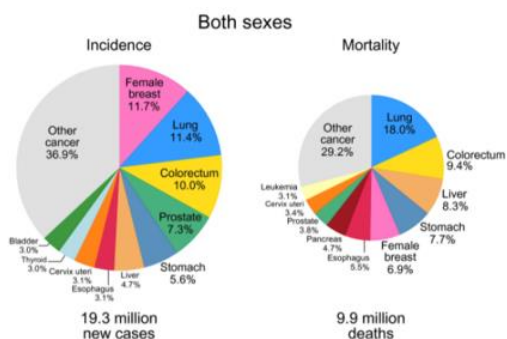


Figure 1: Cancer death rate statistics (Sung et al., 2021)

Non-small cell lung cancer and small cell lung cancer are the 2 main kinds of lung cancer (NSCLC). Non-small cell lung cancer (85% of cases) has a wide range of histological subtypes, including adenocarcinoma, large cell carcinoma, and squamous cell carcinoma. The two most often mutated genes in non-small cell lung cancer patients are epidermal growth factor receptor (EGFR, HER1, or c-ErbB-1) and anaplastic lymphoma kinase (ALK), which frequently manifests as a fusion product with another gene: an echinoderm microtubule-associated protein-like 4 (EML4). (Lam and Scott, 2018)

By evaluating a large number of crystallographic structures of a given enzyme in a combination with different inhibitors, protein-ligand docking is a technique that adapts knowledge-based pairwise potentials to a protein-specific target function and implicitly takes protein flexibility into account. Several inhibitors are combined with the enzyme. A protein-ligand docking technique must include both sampling and scoring. The generation of potential ligand-binding orientations or configurations close to a protein's binding site is referred to as sampling, which has

two components: ligand sampling and protein flexibility. (Wang et al., 2021)

Site-specific docking is when the binding residues are defined so that the ligand binds within only the specific pocket. According to Figure 02 below, the receptor employed in this study is "Epidermal Growth Factor Receptor Tyrosine Kinase Domain with 4-Anilinoquinazoline Inhibitor Erlotinib" and has a PDB ID of 1M17.

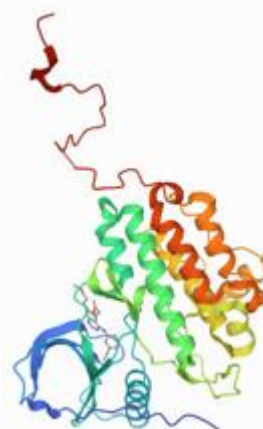


Figure 2: 1M17 receptor

EGFRs (Epidermal Growth Factor Receptors) are transmembrane receptors found on cell membranes that regulate cell development, apoptosis, and other biological processes. Mutations in EGFR can lead to persistent or aberrant activation of the receptor, leading to uncontrolled cell proliferation and malignancies such as non-small cell lung cancer (NSCLC). (Patel and Narechania, 2018) 1M17 is a mutated Epidermal growth factor receptor, so its inhibition can stop cell proliferation.

FDA- approved drugs are employed in this study as standards to see if they could be repurposed for other uses. (Anwaar et al., 2022)


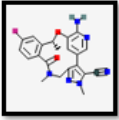
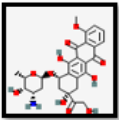
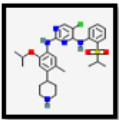

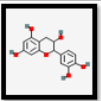
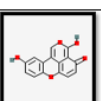
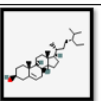
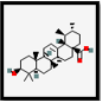
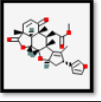
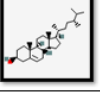
FDA Approved Drugs	PubChem ID/ZINC ID	2D Structure	Reference
A-1331852	71565985		(Wang <i>et al.</i> , 2020)
Lorlatinib	71731823		(Shaw <i>et al.</i> , 2020)
Doxorubicin	31703		(Melguizo <i>et al.</i> , 2015a)
Caritinib	57379345		(Shaw <i>et al.</i> , 2014)
Nilotinib	644241		(Go <i>et al.</i> , 2013)

Table 1: FDA Approved Drugs

Phytochemical	Natural source	PubChem ID/ZINC ID	2D Structure	Reference
Catechins	Green tea	1203		(Zhong <i>et al.</i> , 2012)
Sorastolonin B	Scirtus vagans	135659042		(Tang <i>et al.</i> , 2018)
Phytosterols	Fruits and vegetables	12303662		(O'faller and Snyder, 2012)
Ursolic Acid	Fruits and herbs	64945		(Kang <i>et al.</i> , 2021)
Nimbolide	Neem seed extracts	12313376		(Rahal, Kumar and Malik, 2021)
Campesterol	Elephantopus scoticus, and Eugenia vertina	173183		(Jiang <i>et al.</i> , 2019)

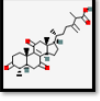
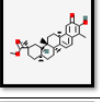
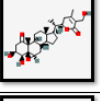
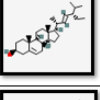
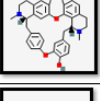
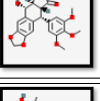
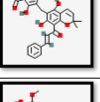
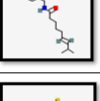
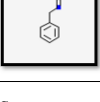
Zincnic acid A	Taiwanofungus camboratus	10004842		(Paravarga Matsuda <i>et al.</i> , 2021)
Estriol	Celastraceae and Hippocratic	159516		
Viscosalactone B	Physalis peruviana, Withania somnifera, and Physalis longifolia	57403080		
Stigmasterol	fats and oils of soybean, calabar bean and rape seed	5280794		(Deng <i>et al.</i> , 2021)
Berberine	Berberis species shrubs leaves	275182		(Liu <i>et al.</i> , 2021)
Podofilox	Coniferaceae and Berberidaceae plants	10607		(Ardalami, Avan and Ghayour-Mobarhan, 2017)
Rottlerin	Mallotus philippinensis plant	5281847		(Ma <i>et al.</i> , 2018)
Capsaicin	In all chili peppers	1548943		(Amundakumar <i>et al.</i> , 2015)
Benzyl isothiocyanate	Mustard plant Alliania petiolata, seeds of the pila tree (Salvadora persica), and papaya (Carica papaya) seeds	2346		(Zhang <i>et al.</i> , 2017)

Table 2: Phytochemicals

Redocking and Ramachandran's plot are two validation techniques, used for the validation of the results gained in protein-ligand docking.

The Ramachandran plot can be used to evaluate the accuracy of protein structure prediction. This is done by using torsion angles to calculate the characteristics of the protein, before and after docking. (Agnihotry *et al.*, 2022)

In addition to the accuracy and speed of sampling and counting, the ability to dock with approved binding sites is another important factor to consider when

choosing a docking tool for real-world applications. When the ligand and protein are delivered in the correct bound conformation, redocking is the simplest example. This not only avoids the general requirement to adapt at least the conformations of the ligand and protein side chains to form the correct complex, but it also makes it much easier to accurately assess the correct complex than identifying a complex with one or more functional groups is out of place, as is the case with docking. (Zavodszky and Kuhn, 2006). The significance of this study is that despite recent breakthroughs in the treatment of NSCLC, SCLC patients still have few treatment options. Many technical, pharmacological, and service advances have been made in the diagnosis and treatment of lung cancer over the past ten years, but challenges remain regarding their best use and cost-effectiveness. Thus, the treatment techniques cannot be considered, for widespread use, even though they hold, mildly effective results so far. (Jones and Baldwin, 2018)

Objectives

To identify the best ligands and their binding sites against lung cancer receptors. To familiarize with software such as AutoDock, Chimera, PyMOL, Open Babel GUI, and BIOVIA Discovery Studio. To identify the best effective FDA-approved drugs and their binding sites against lung cancer receptors site-specific docking and to identify potent phytochemicals and their binding sites against lung cancer using site-specific docking.

Materials

Hardware used this study consists of a PC with an 8th Gen Intel processor, and an Intel (R) Core (TM) i7-8550U CPU @ 1.80GHz, along with a 12 GB RAM and Windows 11 operating system. Software used were Autodock 4.2.6, Open Babel

GUI 2.4.1 and BIOVIA Discovery Studio (DS) Visualizer 21.1.1.0.0. MGL Tools 1.5.7 and Python 3.10.0 were also downloaded, as support to help run the Autodock 4.2.6 software. The web tools incorporated were NCBI PubChem database, Research Collaboratory for Structural Bioinformatics Protein Data Bank (RCSB PDB) and ADMETlab 2.0. Using PDB, the three-dimensional structure of the receptor Epidermal Growth Factor Receptor Tyrosine Kinase Domain with 4-Anilinoquinazoline Inhibitor Erlotinib (PDB ID: 1M17) was obtained, to go alongside the ligands obtained through NCSB Pubchem.

METHODOLOGY

Epidermal Growth Factor Receptor tyrosine kinase domain with 4-anilinoquinazoline inhibitor erlotinib (PDB ID: 1M17) and Crystal Structure of BCL-XL bound to BM501 (PDB ID: 3SPF) was downloaded from RCSB PDB in PDB format. Then, the 3D structures of FDA-approved drugs and phytochemicals were retrieved in SDF format from NCBI PubChem and converted to PDBQT using Open Babel GUI. Afterwards, water molecule and Hetero-atoms removal took place first, followed by repairing of missing atoms the, along with the addition of polar hydrogens and Kollman charges. After the addition of Kollmann's charges, the total charge on residue was checked and the charge deficit was spread. Following this, the ligand was added as PDBQT file. For the setting of grid parameter, macromolecule pdbqt file was chosen, followed by the choosing of the ligand. Parameters were set by gaining the amino acid residues from using Castp website and the grid box was formed. The active amino acid residues in the binding pocket retrieved using CASTp were ASP783, ASN784, GLN958, ARG962, MET963, HIS964, LEU977, MET978, ASP979, GLU980, ASP982, MET983,

ASP984, and VAL986 of the receptor and the center grid box values; X (20.663), Y (0 4.2060), and Z (56.92), with the grid sizes for X, Y and Z all being 40, along with a spacing of 0.375Å° (Figure 03). Thus, enveloping the chosen binding site. Then, the grid file was then saved as .GPF file and auto grid was executed.

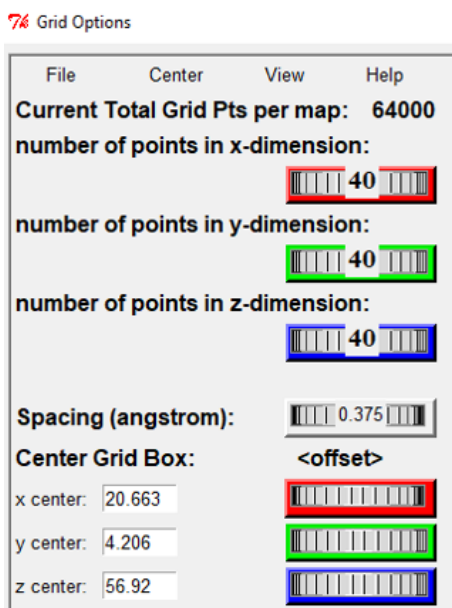


Figure 3: Grid box parameters

The commencement of the docking procedure begins, with the macromolecule and ligand being chosen. Then genetic algorithm was set to 10 GA runs and 150 populations. Finally, output Lamarckian GA was selected and saved as .DPF file, followed by running AD4. For analysis, the .DLG file of the Protein-Ligand docking, was selected, after the confirmation of RMSD data table was analyzed for BE and Ki.To gain a visualization of the interactions and poses of the docked site UCSF Chimera and BIOVA DS was used. The docking pose was obtained from Chimera 1.16, from (Docked_complex.pdb), along with using enhancements such as Interactive Ribbons

I and Publication 3, as the presets. Interactions were visualized from BIOVIA DS. This was done by opening by converting the docked complex file which is saved a .PDBQT file into a .PDB file using Open Babel GUI. Next, the docked .PDB file was opened in BIOVIA DS and to gain a visual of the interactions, 2D diagrams is selected and the interactions will appear. The interactions are analyzed with respect to Hydrogen (H-bond) Bonds and Hydrophobic bonds. Analysis of ADMET properties of phytochemical takes place Phytochemical canonical SMILES were added to the ADMET LAB 2.0 from PubChem and drug-likeness, absorption, lipophilicity ADMET parameters were analyzed. Lipinski's rule of 5 was applied to drug-likeness(Venkataramanan Swaminathan, Nur Ain Bt Rodzi, 2021)

For validation, Ramachandran Plot and Superimpose were used. In Ramachandran plot, the PDB files of the receptor before and after docking, were used to generate Ramachandran plots, using PROCHECK V6. In PyMOL, the redocked file of 1M17 receptor and its natural ligand (AQ4) were aligned and the superimposed structure is visualized and the RMSD value it is correlated with is obtained.

RESULTS

FDA Approved Drugs-1M17		
	Docking Parameters	
Ligand (FDA-approved Drugs)	Binding Energy (kcal/mol)	Inhibition Constant (µM)
A-1331852	-7.89	1.64
Ceritinib	-7.67	2.40
Nilotinib	-8.37	731.36×10^{-3}
Lorlatinib	-6.43	19.49
Doxorubicin	-7.21	5.23

Table 7: 1M17 FDA approved drugs results

Out of the 15 phytochemicals that were docked in this study, only 10 were further studied and 5 others rejected. This was due to 5 of the phytochemicals having a lower than optimal binding energy of above -5 kcal/mol.

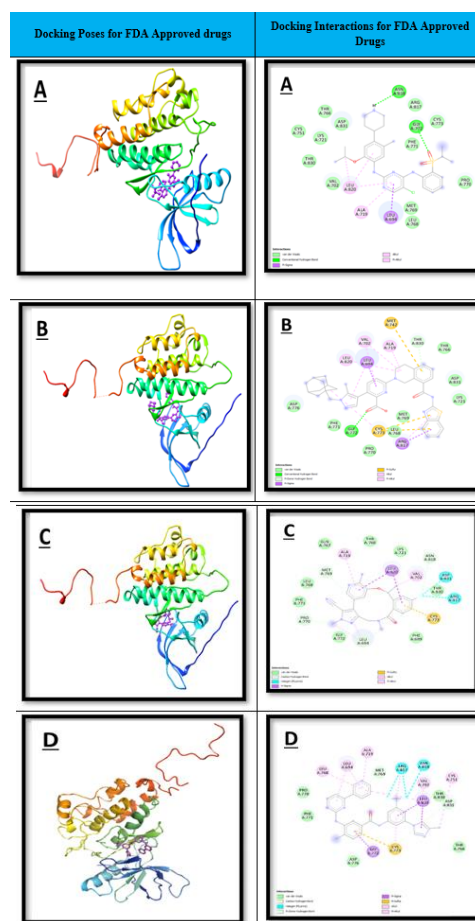
Phytochemical- IM17 (Accepted)		
Ligands	Binding Energy (kcal/mol)	Inhibition Constant (μM)
Catechins	-5.19	155.8
Sparstolonin B	-7.01	7.22
Phytosterols	-9.87	58.05×10^{-3}
Ursolic Acid	-12.56	620.13×10^{-4}
Nimbolide	-7.95	1.49
Campesterol	-8.95	274.92×10^{-3}
Zhankuic acid A	-9.67	81.36×10^{-3}
Pristimerin	-8.02	1.33
Viscosalactone B	-8.46	631.04×10^{-3}
Stigmasterol	-9.08	219.36×10^{-3}

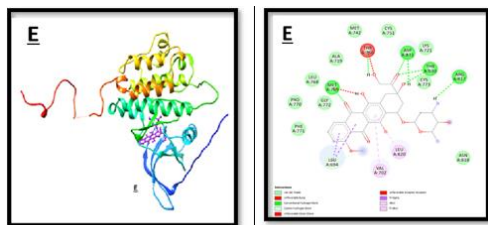
Table 8: IM17 Phytochemicals results (Accepted)

Phytochemical- IM17 (Rejected)		
Ligands	Binding Energy (kcal/mol)	Inhibition Constant (μM)
Berberamine	-3.44	2.99×10^3
Podofilox	-3.89	1.41×10^3
Rottlerin	-2.24	22.63×10^3
Capsaicin	-3.77	1.7×10^3
Benzyl isothiocyanate	-4.64	1.09×10^3

Table 9: Phytochemicals results (Rejected)

The most effective FDA approved drug for the Epidermal Growth Factor Receptor tyrosine kinase domain with 4-anilinoquinazoline inhibitor erlotinib receptor is Nilotinib, with the lowest binding energy and also the lowest inhibition constant. Among the phytochemicals the most effective of the accepted phytochemicals was Ursolic Acid, which has the best binding energy and inhibition constant. Although, the phytochemicals Phytosterols, Zhankuic Acid A and Stigmasterol have great potential as well, with binding energies between -9 to -10 kcal/mol and also having nano-molar (nM) inhibition constants.





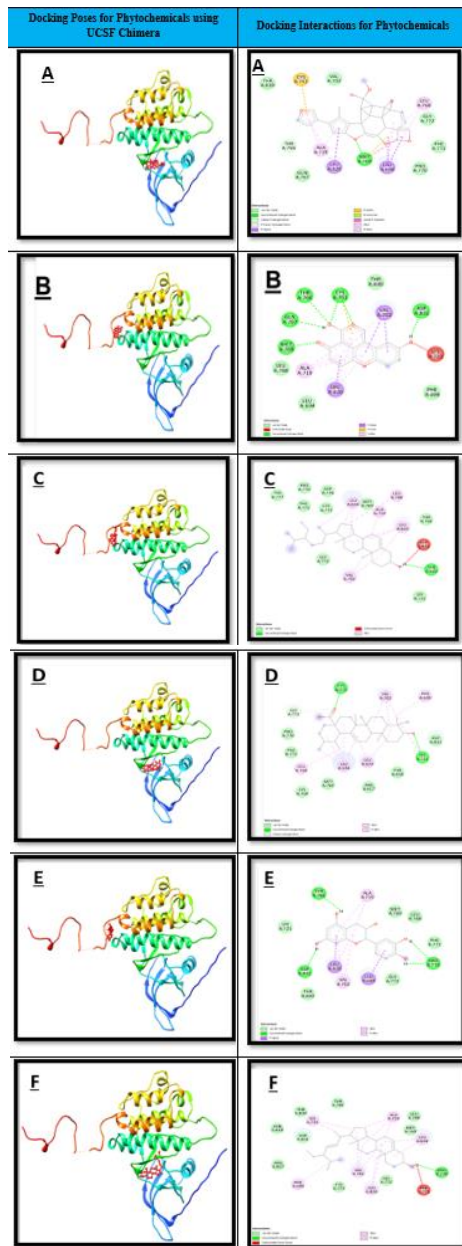
A- Certinib, B- A-1331852, C- Lorlatinib, D- Nilotinib and E- Doxorubicin

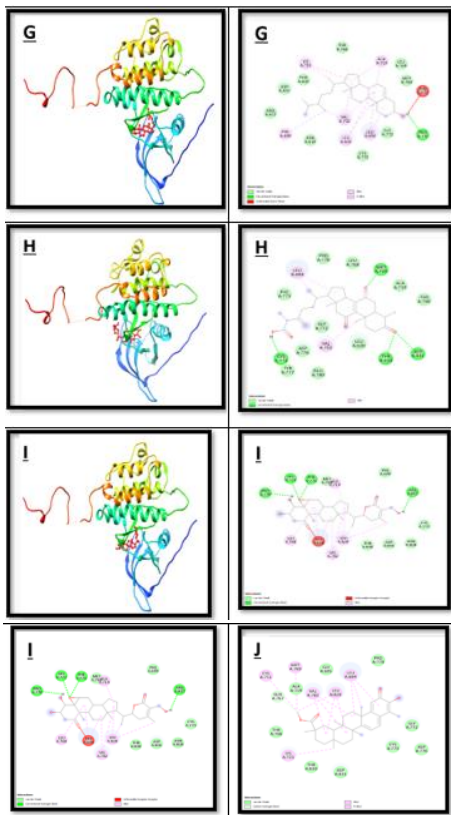
Table 10: IM17 Docking poses and Interactions visualized- FDA approved drugs

IM17 SITE SPECIFIC INTERACTION- FDA		
Ligand	H- Bond	Hydrophobic Bond
A-1331852	GLY 772	THR 766, THR 830, ALA 719, VAL 702, LEU 694, LEU 820, ASP 776, PHE 771, PRO 770, CYS 773, LEU 768, ARG 817, MET 769, LYS 721, ASP 831
Doxorubicin	SER 164, VAL 161	ARG 163, VAL 163, SER 25, LEU 17, VALL 155, SER 23, TRP 24, TYR 22, GLN 160, GLU 158, MET 159
Lorlatinib	-	ASN 818, LYS 721, THR 766, ALA 719, GLN 767, MET 769, LEU 768, PHE 771, PRO 770, GLY 772, LEU 694, PHE 699, CYS 773, ARG 817, THR 830, ASP 831, VAL 702, LEU 820
Certinib	ASN 818, GLY 772	CYS 773, ARG 817, THR 766, ASP 831, LYS 721, CYS 751, THR 830, VAL 702, LEU 820, ALA 719, LEU 694, MET 769, LEU 768, PRO 770, PHE 771
Nilotinib	-	ASN 818, ARG 817, MET 769, ALA 719, LEU 694, LEU 768, PRO 770, PHE 771, ASP 776, GLY 776, GLY 772, CYS 773, THR 766, LEU 820, ASP 831, THR 830, CYS 751, VAL 702

GLY 772 was identified as the most common amino acid residue, with respect to H-bonds and hydrophobic bonds.

Table 12: IM17 phytochemicals poses and interactions





A- Nimbolide, B- Sparstolonin B, C- Phytosterol, D- Ursolic Acid, E- Catechins, F- Stigmasterol, G- Campesterol, H- Zhankuic Acid A, I- Viscosalactone B and J- Pristimerin

Table 13: IM17 site specific Interactions- Phytochemicals

IM17 site specific Interactions- Phytochemicals		
Ligand	Hydrogen bonds	Hydrophobic bonds
Ursolic acid	CYS 773, LYS721	PRO 770, PHE 771, LYS 704, MET 769, ARG 817, THR 830, ASP 831, VAL 702, PHE 699, LEU 768, LEU 694, LEU 820
Phytosterols	THR830	TYR 777, PRO 770, ASP 776, PHE 771, CYS 773, MET 769, THR 766, LYS 721, GLY 772, LEU 694, ALA 719, LEU 768, LEU 820, VAL 702
Nimbolide	MET769	THR 830, VAL 702, GLY 772, PHE 771, PRO 770, GLN 767, ALA 719, LEU 768, LEU 694, LEU 820, CYS 751
Sparstolonin B	MET769, GLN767, THR766, CYS751, ASP831,	THR 830, LEU 694, PHE 699, LEU 768, VAL 702, LEU 820, ALA 719
Campesterol	PRO 770	LEU 694, PHE 699, VAL 702, ALA 719, LYS 721, THR 766, LEU 768, MET 769, GLY 772, CYS 773, ARG 817, ASN 818, THR 830, ASP 831
Stigmasterol	PRO 770	LEU 694, PHE 699, VAL 702, ALA 719, THR 766, LEU 768, MET 769, GLY 772, CYS 773, ARG 817, ASN 818, LEU 820, THR 830, ASP 831
Catechins	PRO 770, ASP 831, THR 766	ALA 719, LYS 721, THR 830, LEU 820, VAL 702, LEU 694, GLY 772, PHE 771, LEU 768, MET 769
Zhankuic acid A	CYS 773, MET 769, THR 830, ASP 831	PRO 770, LEU 694, PHE 771, GLY 772, ASP 776, TYR 777, GLU 780, LEU 820, THR 766, ALA 719, VAL 702
Pristimerin	-	PRO 770, LEU 694, PHE 771, GLY 772, ASP 776, TYR 777, GLU 780, LEU 820, THR 766, ALA 719, MET 769, THR 830, VAL 702
Viscosalactone B	ARG 817, PHE 771, GLY 772, PRO 770	PHE 746, ALA 149, PHE 105, VAL 126, ALA 104, LEU 108, PHE 97, ALA 142, TYR 101, LEU 130, GOL 212, GLU 129, THR 830, VAL 702

VAL 702 and THR 830 were the most common amino acid residues present, with respect to H-bond and hydrophobic bonds.

Phytochemicals	Lipinski Rule	TPSA	CYP 2C19	CYP 2C9	CYP 3A4	Caco2	BBB	MDCK	Protein Plasma binding	Log P
Ursolic Acid	Accepted	57.53	No	No	No	-5.396	No	1.00E-05	97.44%	6.453
Phytosterols	Accepted	20.23	No	No	No	-4.713	No	1.30E-05	93.74%	7.899
Catechins	Accepted	110.38	No	No	No	-5.971	No	4.30E-06	92.07%	1.142
Sparstolonin B	Accepted	83.81	No	No	No	-4.842	No	7.90E-06	89.60%	3.148
Nimbolide	Accepted	92.04	No	Yes	Yes	-5.338	Yes	4.10E-05	91.29%	2.176
Campesterol	Accepted	20.23	No	No	No	-4.65	No	1.10E-05	93.93%	7.735
Zhankuic acid A	Accepted	88.51	No	No	No	-5.15	Yes	1.40E-05	94.16%	4.404
Pristimerin	Accepted	66.76	No	No	Yes	-5.063	No	2.20E-05	98.51%	5.65
Viscosalactone B	Rejected	195.74	No	No	No	-5.902	No	5.90E-05	48.01%	1.692
Stigmasterol	Accepted	20.23	No	No	Yes	-4.576	No	1.40E-05	88.12%	7.5

Figure 4: ADMET properties for phytochemicals table Abbreviations-TPSA: total prostate-specific antigen, CYP 2C19: Cytochrome P450 2C19, CYP 2C9: Cytochrome P450 family 2 subfamily C member 9, CYP 3A4: Cytochrome P450 3A4, Caco2: Immortalized cell line of human colorectal adenocarcinoma cells, BBB: Blood brain barrier, MDCK: Madin-Darby canine kidney and Log P:

The logarithm (base 10) of the partition coefficient (*P*).

Drug similarity is a delicate balance between many structural and molecular characteristics that determine whether a given molecule is a drug or not. The behavior of a molecule in a living organism is influenced by these properties, in particular lipophilicity, electronic distribution, hydrogen bonding properties, the size and flexibility of the molecule, and the presence of various pharmacophoric properties. These characteristics include transport, protein affinity, reactivity, toxicity, metabolic stability, and etc. (Turner and Agatonovic-Kustrin, 2006)

A physicochemical property called lipophilicity, which describes the ability of a molecule to break down into octanol or water, is often considered extremely important for absorption rates. The logarithm of the drug distribution in the organic phase relative to the aqueous phase, or log*P*, is used to determine lipophilicity. (Ivanović et al., 2020) Therapeutic agents usually consist of small molecules that comply with Lipinski's rule of five (i.e., a log *P* partition factor of no more than 5) and satisfy other criteria. (Goodwin, Bunch and McGinnity, 2017). Through passive diffusion, the BBB provides a flow of chemicals such as glucose and amino acids that are essential for brain function, as well as water, certain gases, and fat-soluble compounds. The BBB (Blood brain barrier) protects the brain from various common bacterial diseases. (Fong, 2015)

Topological polar surface area (TPSA), which uses functional group contributions based on a large database of structures, is an easy way to calculate polar surface area without the need to determine the required biological conformation or conformations or the three-dimensional structure of the ligand. The sign of the TPSA coefficient

can indicate whether a more polar ligand is preferred to increase activity. (Prasanna and Doerksen, 2008) Usually, only phytochemicals over 90 Å² can permeate the BBB, but since it is already confirmed that none of the phytochemicals listed in the ADMET table is able to pass through, showing that the phytochemicals cannot reach the brain or effect the central nervous system.

Redocking result			
Binding Energy (kcal/mol)	Inhibition constant	Receptor	Natural ligand
-6.15	31.06 μM	1M17	AQ24

Table 14: Redocking results

Superimposed result		
Receptor	Natural Ligand	RMSD
1M17	AQ4	1.309 Å

Table 15: Superimpose results

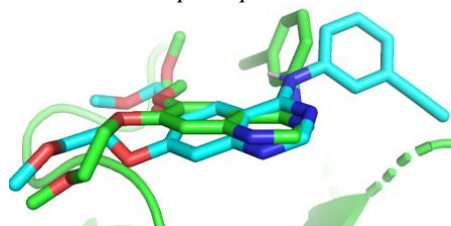


Figure 5: 1M17-AQ4 redocking

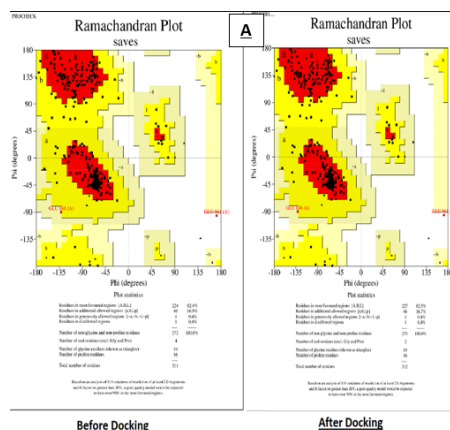


Figure 6: Ramachandran plot- 1M17 A- Before docking and B- After docking

The percentage of residues in most favored regions is almost equal from before and after docking, with only a 0.1% difference between the two. 96.05% in residues in most favored region before docking, and 96.04% after docking.

DISCUSSION

In docking programs, most conformational optimization techniques are able to address only one specific goal, such as binding energy, shape complementarity, or chemical complementarity. A sufficient solution to the whole problem cannot be discovered by using individual optimization algorithms with a single goal, because real-world situations usually involve many goals (potentially conflicting ones) or optimization criteria that must be met simultaneously. (Li et al., 2009)

The flexibility of both the ligand and the receptor must be taken into account, since in this situation both will change their conformations to form an ideally suited minimum energy complex. When the receptor is also flexible, the price is very high. Because the receptor remains rigid during docking, which represents a compromise between accuracy and computational time, is to treat the ligand as flexible. To represent the flexibility of the ligand while maintaining the rigidity of the receptor, Autodock 4.0 uses evolutionary, genetic, and Lamarckian genetic algorithm techniques. (Meng et al., 2012)

There were no sidechains present in 1M17 receptor. As such there was no need for deletion of sidechains. In AD4's energy estimation function, the calculation of pairwise atomic terms includes estimates of various secondary interactions, dispersion/repulsion, hydrogen bonding, electrostatics, and desolvation. Thus, the

calculation of the exact partial charges of the ligand and protein is expected to have a strong impact on both the docking conformation and the energy estimate of the resulting complex, possibly leading to a more accurate estimate of the complex geometry and binding energy. The AutoDockTools program allows the user to use empirical charge calculations, combined Gasteiger or Kollman's charges. However, this charge calculation method has been shown to give less accurate partial charges than semi-empirical methods. (Bikadi and Hazai, 2009). The ability of docking programs to mimic the way ligands bind as seen in the bonded crystal structure, which is typically assessed by calculating the root mean square distance (RMSD) between the non-hydrogen atoms of the ligand in the crystal structure and the corresponding atoms in the docked pose. If a number is defined below which a pinned pose is considered correct, this can be achieved using the RMSD metric used in docking evaluation. A measure of docking performance is the frequency of such successful docking positions in the data set. It is generally accepted that the threshold value of RMSD equal to 2.0 Å makes it possible to distinguish between successful and unsuccessful replication in the binding mode. (Yusuf et al., 2008)

In superimposing the receptor 1M17 RMSD value of 1.309 Å was recorded, which is not a perfect result. However, the receptor ability as an inhibitor cannot be mistaken, with good docking results, across all docking techniques used. Despite its widespread use, the calculation of RMSD is still associated with a number of difficulties. Symmetry problems appear at the level of protomers in macromolecular complexes. Most of the proteins found in the PDB are oligomeric complexes composed of two or more subunits that work together to create rotational or helical symmetry. According to crystallographic point group operations,

protein assemblies with rotational symmetry are divided into cyclic groups (Cn), dihedral groups (Dn), and icosahedral groups (In). The most common of the three examples in PDB are cyclic groups, consisting of a single axis of rotation and a ring of ordered subunits. Since the RMSD becomes rotationally invariant, imposing complexes with perfect rotational symmetry is problematic. However, the symmetry in biomolecules is rarely perfect and is often broken by functionally important conformational shifts. (Rueda et al., 2013)

A protein is often prepared for a virtual screening calculation by removing all water from the binding site. An enormous and unreasonable number of options can result from docking in all possible water configurations. It is clear that there is a trade-off between accuracy and speed when considering these water molecules during docking calculations. (Wong and Lightstone, 2011). Hydrogen bonds with water molecules are broken during ligand binding and new hydrogen bonds are formed between the protein and the ligand. Thus, a new technique is used to evaluate the change in hydrogen binding energy during the binding process, often known as the hydrogen bonding penalty. The hydrogen bond penalty can be used to increase the accuracy of mandatory energy calculations, in addition to filtering out implausible docking stations. (Zhao and Huang, 2011)

Flexible ligand-receptor docking using a Lamarckian genetic algorithm (LGA) version that supports a large number of degrees of freedom in the ligand's location. As a result, greater outcomes can be obtained in less time. (Fuhrmann et al., 2010). In most of the cases, barring a few abnormalities, site specific results have been proven have better binding affinity, than blind dockings. Intermolecular interactions, solvent effects, and the dynamics of the protein-ligand complex all affect its strength. Thus, molecular

docking uses scoring algorithms to provide a fast and rough calculation of binding affinity to avoid the significant computational cost associated with this simulation. (Pantsar and Poso, 2018). The FDA approved drug Doxorubicin, shows less than ideal results for docking with 1M17 receptor. This could be due to the drug being an inhibitor or small cell lung cancer, instead of non-small cell lung cancer. The pathway it inhibits is the signaling pathway of TGF- β 1, (Melguizo et al., 2015b) whose upregulation, causes metastasis, while 1M17 receptor pathway is signal transduction pathway.

The receptor 1M17 is also a receptor for not just Lung cancer but is also an epidermal growth factor receptor for breast cancer. It is a EGFR-erlotinib. (Haghighijoo et al., 2018) It could thus be theorized, that phytochemicals and drugs that inhibit the receptor for lung cancer, may also have an inhibitory affect for breast cancer patients as well.

1M17 result comparison				
Phytochemicals	Reference Results- (Patel and Narechania, 2018b)		Gained Results	
	Binding Energy (kcal/mol)	Inhibition Constant (μ M)	Binding Energy (kcal/mol)	Inhibition Constant (μ M)
Ursolic Acid	9.186	$231.57 \times 10^{-3} \mu$ M	-12.56	620.13×10^{-4}
Campesterol	9.085	$219.082 \times 10^{-3} \mu$ M	-8.95	274.92×10^{-3}
Stigmasterol	9.048	233.20×10^{-3}	-9.08	219.36×10^{-3}

Table 16: 1M17 results comparison

Reference results gained by an article for Ursolic Acid docking of the 1M17 receptor, have been proved to be better in this research than when done, during the experiment. This could be due to, a different approach used in the methodology of gaining the molecular docking. However, results gained for Campesterol and Stigmasterol were both less than, the referenced results.

1M17 result comparison		
Phytochemicals	Reference Results- (Patel and Narechania, 2018b)	Gained Results
	Amino Acid Residues	Amino Acid Residues
Ursolic Acid	LEU 694, GLY 695, SER 696, GLY 697, PHE 699, VAL 702, ALA 719, ILE 720, LYS 721, GLU 738, MET 742, LEU 764, ILE 765, THR 766, CYS 773, ARG 817, LEU 820, THR 830, ASP 831	PRO770, PHE771, LYS704, MET769, ARG817, THR830, ASP831, VAL702, PHE699, LEU768, LEU694, LEU820, CYS773, LYS721
Campesterol	LYS 692, LEU 694, VAL 702, ALA 719, ILE 720, LYS 721, MET 742, LEU 764, THR 766, LEU 768, MET 769, PRO 770, GLY 772, CYS 773, LEU 820, THR 830, ASP 831	LEU 694, PHE 699, VAL 702, ALA 719, LYS 721, THR 766, LEU 768, MET 769, GLY 772, CYS 773, ARG 817, ASN 818, THR 830, ASP 831, PRO 770
Stigmasterol	LYS 692, LEU 694, VAL 702, ALA 719, ILE 720, LYS 721, GLU 738, MET 742, LEU 764, ILE 765, THR 766, LEU 768, MET 769, PRO 770, GLY 772, CYS 773, LEU 820, THR 830, ASP 831, PHE 832	LEU 694, PHE 699, VAL 702, ALA 719, THR 766, LEU 768, MET 769, GLY 772, CYS 773, ARG 817, ASN 818, LEU 820, THR 830, ASP 831, PRO 770

Table 17: 1M17 Results comparison for amino acid residues

created. In order to develop rules for detection, set thresholds correctly, and be able to interpret results, it is important to know the energetic contributions of biologically significant interactions, their preferred atomic types, and distances and angles. (Salentin et al., 2014) Among the amino acid residues present in both the referenced and gained results, it can be noted that the most common residue, among all 6 of them are LEU 694 and VAL 702. The next most common was LEU 820, which was found in all other results, except for the gained Campesterol result. This can be seen in the table above.

Hydrogen- bonds can be seen in all 3 of the gained results (CYS773, LYS721, PRO 770). In general, H-bonds are believed to facilitate protein-ligand interaction. To create stronger protein-ligand interactions, H-bond donors or acceptors are usually introduced; however, this often prevents a net increase in binding affinity. Hydrogen bonds are also reported to increase ligand binding affinity by pushing protein-bound water molecules into the solvent bulk rather than focusing on protein-ligand interactions. (Chen et al., 2016) Thus, as stated above binding affinity increases, when h-bonds are reported, as such the results can be considered to be favorable for drug making of anti-cancer drugs.

These altered hydrophobic interactions help stabilize the biochemical parameters of the target-drug complexes and improve the binding affinity and biological activity of the complex molecules. (Varma et al., 2010)

CONCLUSION

In conclusion, through AD4 docking and Vina the best FDA approved drugs and phytochemicals can be considered, for 1M17 receptor, using BE, BA and amino acid residue interactions. FDA drugs, A-1331852 is the best approved drug from the sample set for the receptor. The phytochemicals, Ursolic acid, campesterol and stigmasterol were identified to have good docking performances in both AD4 and vina for 1M17. Along with these 3, other efficient bindings for 1M17 are Zhankuic acid A, Viscosalactone B and Stigmasterol. MET 769, PRO 770, THR 830 and GLY 772 were most common amino acid residues for 1M17. Thus, this study proposes, that the lead phytochemicals found in this study, be used as leads for anti-cancer drug development for lung cancer.

For future work, the EFGR receptor 1M17 being used, could be mutated for varying patients, some methods used in molecular docking or MD simulation to predict TKI sensitivity of EGFR mutations have been reported. (Ikemura et al., 2019) Mutation of EFGR can be tested using MD simulations. To relate the biological activity of substances, to the structural characteristics of ligands, such as hydrophobic, electronic, steric and topological parameters, quantitative structure-activity ratio (QSAR) models will be developed. (Gromiha, Nagarajan and Selvaraj, 2018). Most relevant clinical trials, after docking include methodological errors such as small sample size, short trial duration, and no control or placebo group. It is therefore too

early to draw conclusions about the anti-cancer effects of many phytochemicals; instead, large-scale, carefully controlled clinical trials are needed to confirm the efficacy, side effects, and safety of these compounds before they are used to treat cancer. (Choudhari et al., 2020) It has been proven that the method for calculating non-equilibrium free energy, based on free and open-source software, is not inferior to modern commercial programs. In addition, descriptive workflows, including the technical procedures needed to calculate free energy, will offer a simple method for predicting ligand-protein binding affinity. (Gapsys et al., 2020)

REFERENCE

- Agnihotry, S. et al. (2022) 'Protein structure prediction', in *Bioinformatics*. Academic Press, pp. 177–188. doi: 10.1016/b978-0-323-89775-4.00023-7.
- Anandakumar, P. et al. (2015) 'The Anticancer Role of Capsaicin in Experimentally Induced Lung Carcinogenesis', *Journal of Pharmacopuncture*, 18(2), pp. 19–25. doi: 10.3831/kpi.2015.18.011.
- Anwaar, M. U. et al. (2022) 'Combined deep learning and molecular docking simulations approach identifies potentially effective FDA approved drugs for repurposing against SARS-CoV-2', *Computers in Biology and Medicine*, 141, p. 105049. doi: 10.1016/j.combiomed.2021.105049.
- Ardalani, H., Avan, A. and Ghayour-Mobarhan, M. (2017) 'Podophyllotoxin: a novel potential natural anticancer agent.', *Avicenna journal of phytomedicine*, 7(4), pp. 285–294. Available at: /pmc/articles/PMC5580867/ (Accessed: 4 September 2022).
- Bikadi, Z. and Hazai, E. (2009) 'Application of the PM6 semi-empirical method to modeling proteins enhances docking accuracy of AutoDock', *Journal of Cheminformatics*, 1(1), pp. 1–16. doi: 10.1186/1758-2946-1-15.
- Chen, D. et al. (2016) 'Regulation of protein-ligand binding affinity by hydrogen bond pairing', *Science Advances*, 2(3). doi: 10.1126/sciadv.1501240.
- Choudhari, A. S. et al. (2020) 'Phytochemicals in cancer treatment: From preclinical studies to clinical practice', *Frontiers in Pharmacology*. Frontiers Media SA. doi: 10.3389/fphar.2019.01614.
- Dong, Y. et al. (2021) 'Stigmasterol inhibits the progression of lung cancer by regulating retinoic acid-related orphan receptor C', *Histology and Histopathology*, 36(12), pp. 1285–1299. doi: 10.14670/HH-18-388.
- Fong, C. W. (2015) 'Permeability of the Blood–Brain Barrier: Molecular Mechanism of Transport of Drugs and Physiologically Important Compounds', *Journal of Membrane Biology*, 248(4), pp. 651–669. doi: 10.1007/s00232-015-9778-9.
- Fuhrmann, J. et al. (2010) 'A new Lamarckian genetic algorithm for flexible ligand-receptor docking', *Journal of Computational Chemistry*, 31(9), pp. 1911–1918. doi: 10.1002/jcc.21478.
- Gapsys, V. et al. (2020) 'Large scale relative protein ligand binding affinities using non-equilibrium alchemy', *Chemical Science*, 11(4), pp. 1140–1152. doi: 10.1039/c9sc03754c.
- Go, S. Il et al. (2013) 'Nilotinib-induced interstitial lung disease', *International Journal of Hematology*, 98(3), pp. 361–365. doi: 10.1007/s12185-013-1398-5.
- Goodwin, R. J. A., Bunch, J. and McGinnity, D. F. (2017) 'Mass Spectrometry Imaging in Oncology Drug Discovery', in *Advances in Cancer Research*. Academic Press, pp. 133–171. doi: 10.1016/bs.acr.2016.11.005.
- Gromiha, M. M., Nagarajan, R. and Selvaraj, S. (2018) 'Protein structural bioinformatics: An overview', in *Encyclopedia of Bioinformatics and Computational Biology: ABC of Bioinformatics*. Academic Press, pp.

- 445–459. doi: 10.1016/B978-0-12-809633-8.20278-1.
- Haghighijoo, Z. et al. (2018) 'Structure based design and anti-breast cancer evaluation of some novel 4-anilinoquinazoline derivatives as potential epidermal growth factor receptor inhibitors', *Research in Pharmaceutical Sciences*, 13(4), pp. 360–367. doi: 10.4103/1735-5362.235163.
- Ikemura, S. et al. (2019) 'Molecular dynamics simulation-guided drug sensitivity prediction for lung cancer with rare EGFR mutations', *Proceedings of the National Academy of Sciences of the United States of America*, 116(20), pp. 10025–10030. doi: 10.1073/pnas.1819430116.
- Imyanitov, E. N. et al. (2005) 'Mechanisms of lung cancer', *Drug Discovery Today: Disease Mechanisms*. Elsevier, pp. 213–223. doi: 10.1016/j.ddmec.2005.05.015.
- Ivanović, V. et al. (2020) 'Lipinski's rule of five, famous extensions and famous exceptions', *Popular Scientific Article*, 3(1), pp. 171–177.
- Jiang, L. et al. (2019) 'The Protective Effect of Dietary Phytosterols on Cancer Risk: A Systematic Meta-Analysis', *Journal of Oncology*. Hindawi Limited. doi: 10.1155/2019/7479518.
- Jones, G. S. and Baldwin, D. R. (2018) 'Recent advances in the management of lung cancer', *Clinical Medicine, Journal of the Royal College of Physicians of London*. Royal College of Physicians, pp. s41–s46. doi: 10.7861/clinmedicine.18-2-s41.
- Kang, D. Y. et al. (2021) 'Antitumor effects of ursolic acid through mediating the inhibition of stat3/pd-1 signaling in non-small cell lung cancer cells', *Biomedicine*, 9(3). doi: 10.3390/biomedicine9030297.
- Lam, Y. W. F. and Scott, S. A. (2018) 'Pharmacogenomics in Cancer Therapeutics', in *Pharmacogenomics: Challenges and Opportunities in Therapeutic Implementation*. Academic Press, pp. 123–132. doi: 10.1016/B978-0-12-812626-4.00005-X.
- Li, H. et al. (2009) 'An effective docking strategy for virtual screening based on multi-objective optimization algorithm', *BMC Bioinformatics*, 10(1), pp. 1–12. doi: 10.1186/1471-2105-10-58.
- Liu, L. et al. (2021) 'Berbamine Inhibits Cell Proliferation and Migration and Induces Cell Death of Lung Cancer Cells via Regulating c-Maf, PI3K/Akt, and MDM2-P53 Pathways', *Evidence-based Complementary and Alternative Medicine*, 2021. doi: 10.1155/2021/5517143.
- Ma, J. et al. (2018) 'Tumor suppressive role of rottlerin in cancer therapy', *American Journal of Translational Research*. e-Century Publishing Corporation, pp. 3345–3356. Available at: /pmc/articles/PMC6291697/ (Accessed: 4 September 2022).
- Melguizo, C. et al. (2015a) 'Enhanced antitumoral activity of doxorubicin against lung cancer cells using biodegradable poly(Butylcyanoacrylate) nanoparticles', *Drug Design, Development and Therapy*, 9, pp. 6433–6444. doi: 10.2147/DDDT.S92273.
- Melguizo, C. et al. (2015b) 'Enhanced antitumoral activity of doxorubicin against lung cancer cells using biodegradable poly(Butylcyanoacrylate) nanoparticles', *Drug Design, Development and Therapy*, 9, pp. 6433–6444. doi: 10.2147/DDDT.S92273.
- Meng, X.-Y. et al. (2012) 'Molecular Docking: A Powerful Approach for Structure-Based Drug Discovery', *Current Computer Aided-Drug Design*, 7(2), pp. 146–157. doi: 10.2174/157340911795677602.
- Miller, P. E. and Snyder, D. C. (2012) 'Phytochemicals and cancer risk: A review of the epidemiological evidence', *Nutrition in Clinical Practice*. Nutr Clin Pract, pp. 599–

612. doi:
10.1177/0884533612456043.
- Pantsar, T. and Poso, A. (2018) 'Binding affinity via docking: Fact and fiction', *Molecules*. Multidisciplinary Digital Publishing Institute (MDPI), p. 1DUMMY. doi: 10.3390/molecules23081899.
- Patel, C. N. and Narechania, M. B. (2018a) 'Targeting epidermal growth factor receptors inhibition in non-small-cell lung cancer: a computational approach', *Molecular Simulation*, 44(17), pp. 1478–1488. doi: 10.1080/08927022.2018.1515484.
- Patel, C. N. and Narechania, M. B. (2018b) 'Targeting epidermal growth factor receptors inhibition in non-small-cell lung cancer: a computational approach', *Molecular Simulation*, 44(17), pp. 1478–1488. doi: 10.1080/08927022.2018.1515484.
- Prasanna, S. and Doerksen, R. (2008) 'Topological Polar Surface Area: A Useful Descriptor in 2D-QSAR', *Current Medicinal Chemistry*, 16(1), pp. 21–41. doi: 10.2174/092986709787002817.
- Purawarga Matada, G. S. et al. (2021) 'Molecular docking and molecular dynamic studies: screening of phytochemicals against EGFR, HER2, estrogen and NF-KB receptors for their potential use in breast cancer', *Journal of Biomolecular Structure and Dynamics*. doi: 10.1080/07391102.2021.1877823.
- Rahal, A., Kumar, D. and Malik, J. K. (2021) 'Neem Extract', in *Nutraceuticals: Efficacy, Safety and Toxicity*. Academic Press, pp. 945–958. doi: 10.1016/B978-0-12-821038-3.00056-2.
- Rueda, M. et al. (2013) 'BioSuper: A web tool for the superimposition of biomolecules and assemblies with rotational symmetry', *BMC Structural Biology*, 13(1), pp. 1–9. doi: 10.1186/1472-6807-13-32.
- Salentin, S. et al. (2014) 'Polypharmacology rescored: Protein-ligand interaction profiles for remote binding site similarity assessment', *Progress in Biophysics and Molecular Biology*, 116(2–3), pp. 174–186. doi: 10.1016/j.pbiomolbio.2014.05.006.
- Shaw, A. T. et al. (2014) 'Ceritinib in ALK - Rearranged Non-Small-Cell Lung Cancer', *New England Journal of Medicine*, 370(13), pp. 1189–1197. doi: 10.1056/nejmoa1311107.
- Shaw, A. T. et al. (2020) 'First-Line Lorlatinib or Crizotinib in Advanced ALK - Positive Lung Cancer', *New England Journal of Medicine*, 383(21), pp. 2018–2029. doi: 10.1056/nejmoa2027187.
- Sung, H. et al. (2021) 'Global Cancer Statistics 2020: GLOBOCAN Estimates of Incidence and Mortality Worldwide for 36 Cancers in 185 Countries', *CA: A Cancer Journal for Clinicians*, 71(3), pp. 209–249. doi: 10.3322/caac.21660.
- Tang, Y. M. et al. (2018) 'Inhibition of p38 and ERK1/2 pathways by Sparstolonin B suppresses inflammation-induced melanoma metastasis', *Biomedicine and Pharmacotherapy*, 98, pp. 382–389. doi: 10.1016/j.biopha.2017.12.047.
- Turner, J. V. and Agatonovic-Kustrin, S. (2006) 'In silico prediction of oral bioavailability', in *Comprehensive Medicinal Chemistry II*. Elsevier, pp. 699–724. doi: 10.1016/b0-08-045044-x/00147-4.
- Varma, A. K. et al. (2010) 'Optimized hydrophobic interactions and hydrogen bonding at the target-ligand interface leads the pathways of Drug-Designing', *PLoS ONE*, 5(8). doi: 10.1371/journal.pone.0012029.
- Venkataramanan Swaminathan, Nur Ain Bt Rodzi, S. K. (2021) 'Computational Pharmacokinetic and Docking Analysis of Curcumin and Piperine as Inhibitors of E3 Ubiquitin Ligases for Lung Cancer', *Annals of the Romanian Society for Cell Biology*, 25, pp. 4885–4894. Available at: https://www.researchgate.net/publication/349685814_Computational_Pharmacokinetic_and_Docking_Analysis_of_Curcumin_and_Piperine_as_Inhibitors_of_E3_Ubiquitin_Ligas

- es_for_Lung_Cancer* (Accessed: 25 July 2022).
- Wang, L. et al. (2020) 'Discovery of A-1331852, a First-in-Class, Potent, and Orally-Bioavailable BCL-XL Inhibitor', *ACS Medicinal Chemistry Letters*. American Chemical Society, pp. 1829–1836. doi: 10.1021/acsmchemlett.9b00568.
- Wang, Q. Q., Xu, R. and Volkow, N. D. (2021) 'Increased risk of COVID-19 infection and mortality in people with mental disorders: analysis from electronic health records in the United States', *World Psychiatry*, 20(1), pp. 124–130. doi: 10.1002/wps.20806.
- Wistuba, I. I. and Gazdar, A. F. (2006) 'Lung cancer preneoplasia', *Annual Review of Pathology. Annual Reviews*, pp. 331–348. doi: 10.1146/annurev.pathol.1.110304.100103.
- Wong, S. E. and Lightstone, F. C. (2011) 'Accounting for water molecules in drug design', *Expert Opinion on Drug Discovery*. Taylor & Francis, pp. 65–74. doi: 10.1517/17460441.2011.534452.
- Yusuf, D. et al. (2008) 'An alternative method for the evaluation of docking performance: RSR vs RMSD', *Journal of Chemical Information and Modeling*, 48(7), pp. 1411–1422. doi: 10.1021/ci800084x.
- Zavodszky, M. I. and Kuhn, L. A. (2005) 'Lessons from Docking Validation', *J. Med. Chem.*, 47(517), p. submitted.
- Zhang, Q. C. et al. (2017) 'Benzyl isothiocyanate induces protective autophagy in human lung cancer cells through an endoplasmic reticulum stress-mediated mechanism', *Acta Pharmacologica Sinica*, 38(4), pp. 539–550. doi: 10.1038/aps.2016.146.
- Zhao, H. and Huang, D. (2011) 'Hydrogen bonding penalty upon ligand binding', *PLoS ONE*, 6(6), p. 19923. doi: 10.1371/journal.pone.0019923.
- Zhong, Z. et al. (2012) 'Inhibition of proliferation of human lung cancer cells by green tea catechins is mediated by upregulation of let-7', *Experimental and Therapeutic Medicine*, 4(2), pp. 267–272. doi: 10.3892/etm.2012.580.